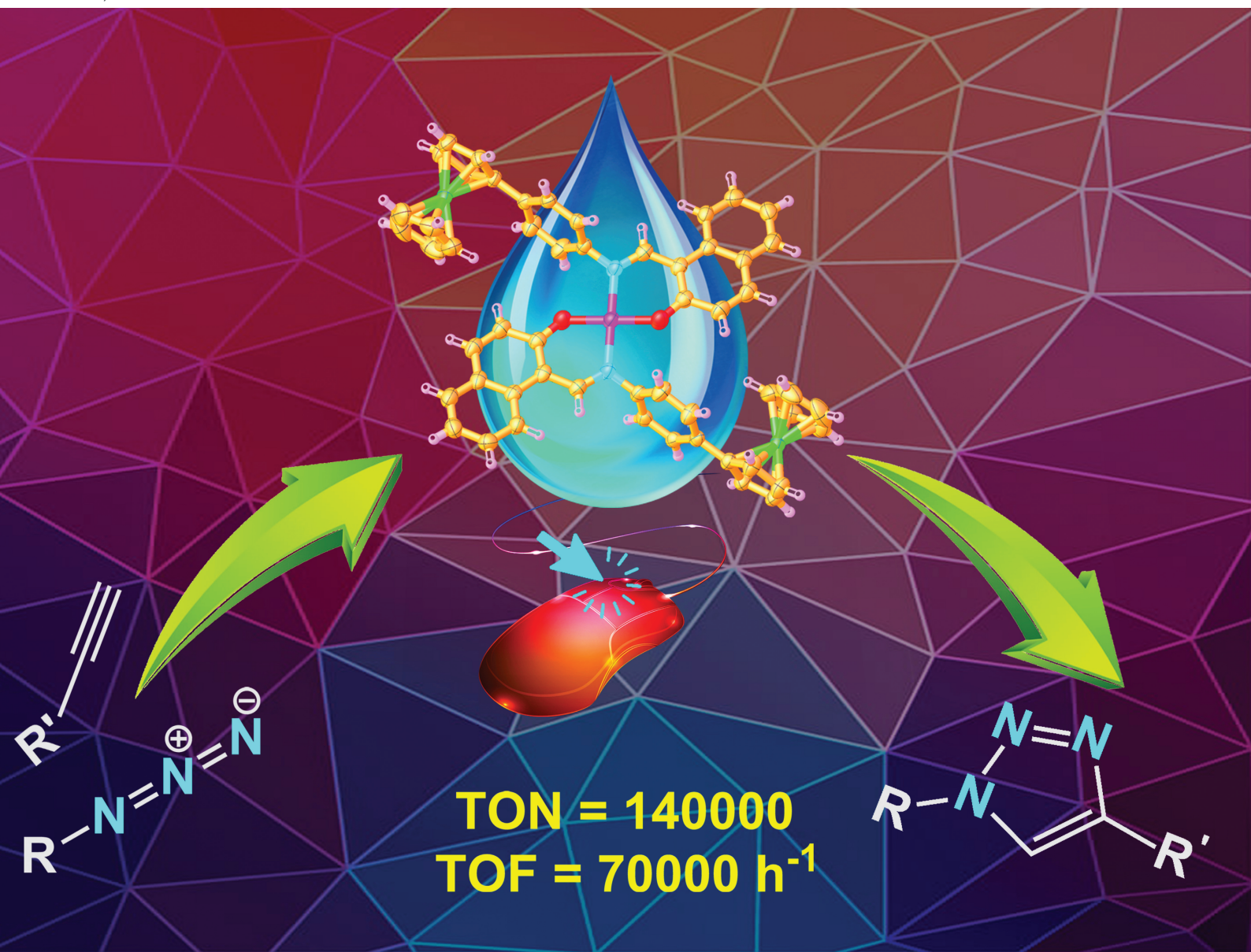


# Dalton Transactions

An international journal of inorganic chemistry

rsc.li/dalton



ISSN 1477-9226

**PAPER**

Biswajit Saha *et al.*

A ferrocene functionalized Schiff base containing Cu(II) complex: synthesis, characterization and parts-per-million level catalysis for azide alkyne cycloaddition

## PAPER



Cite this: *Dalton Trans.*, 2020, **49**, 6578

# A ferrocene functionalized Schiff base containing Cu(II) complex: synthesis, characterization and parts-per-million level catalysis for azide alkyne cycloaddition†‡

Firdaus Rahaman Gayen,<sup>a,b</sup> Abdul Aziz Ali,<sup>a</sup> <sup>a</sup> Debashree Bora,<sup>a,b</sup> Saptarshi Roy,<sup>a</sup> Supriya Saha,<sup>b,c</sup> Lakshi Saikia,<sup>a,b</sup> Rajib Lochan Goswamee<sup>a,b</sup> and Biswajit Saha  <sup>\*a,b</sup>

Atom economy is one of the major factors in developing catalysis chemistry. Using the minimum amount of catalyst to obtain the maximum product yield is of the utmost priority in catalysis, which drives us to use parts-per-million (ppm) levels of catalyst loadings in syntheses. In this context, a new ferrocene functionalized Schiff base and its copper(II) complex have been synthesized and characterized. This Cu(II) complex is employed as a catalyst for popular 'click chemistry', where 1,2,3-triazoles are the end product. As low as 5 ppm catalyst loading is enough to produce gram scale product, and highest turnover number (TON) and turnover frequency (TOF) values of 140 000 and 70 000 h<sup>-1</sup> are achieved, respectively. Furthermore, this highly efficient protocol has been successfully applied to the preparation of diverse functionalized materials with pharmaceutical, labelling and supramolecular properties.

Received 11th March 2020,

Accepted 7th April 2020

DOI: 10.1039/d0dt00915f

rsc.li/dalton

## Introduction

1,2,3-Triazoles are promising N-heterocyclic compounds in medicinal chemistry owing to their efficient amide surrogates.<sup>1</sup> Based on this important structural motif, several drug molecules, like the  $\beta$ -lactam antibiotic tazobactam, broad spectrum cephalosporin antibiotic cefatrizine, anticonvulsant drug rufinamide, and anticancer drug carboxyamidotriazole, are available on the market.<sup>2</sup> However, the chemistry of 1,2,3-triazoles is not confined to medicinal chemistry and has a wide array of applications in modern science and technology including materials science, organic chemistry, polymer chemistry, supramolecular chemistry, and biology, as well as in many industries.<sup>3</sup> Although there are several reports for the synthesis of 1,2,3-triazoles,<sup>4</sup> so far the famous 'click chemistry' approach remains dominant.<sup>5</sup> Sharpless and Meldal are the pioneers of

the Cu-catalysed azide alkyne cycloaddition reaction (CuAAC) for the synthesis of 1,2,3-triazoles, which afforded spectacular advantages like a high regioselectivity, notable atom economy, mild reaction conditions and high yield of the products.<sup>6</sup>

Any copper source that produces catalytically active Cu(I) species, such as both Cu(II) and Cu(I) salts, preformed Cu(I) complexes, metallic copper, Cu-nanoparticles and other Cu-based heterogeneous systems, can be used as a precatalyst in the CuAAC reaction.<sup>7</sup> The most convenient catalytic system is the combination of CuSO<sub>4</sub>·5H<sub>2</sub>O and sodium ascorbate in aqueous media, identified as the Sharpless-Fokin catalyst.<sup>6</sup> Despite its remarkable catalysis, there is a need to use quite large quantities of CuSO<sub>4</sub>·5H<sub>2</sub>O and sodium ascorbate to achieve solely the 1,4-regioisomer in short period of time.<sup>8</sup> This creates a serious concern regarding the complete removal of copper ions, which obstructs its enormous applications in the pharmaceutical industry as well as in biology.<sup>9</sup> To address this problem, recently Uozumi and co-workers reported a reusable, metalloprotein-inspired polymeric Cu(II) catalyst at the parts-per-million (ppm) level for CuAAC reactions in 'BuOH/H<sub>2</sub>O'.<sup>10</sup> Similarly, Astruc *et al.* described the efficient catalytic behaviour of an amphiphilic recyclable dendrimer nanoreactor for the ppm level of the Cu(I) catalysed click reaction in water.<sup>11</sup> In 2016, a new recyclable tris(triazolyl)-poly(ethylene glycol)-based Cu(I) catalyst at the ppm level was reported for accelerating the click reaction in water under an inert atmosphere.<sup>12</sup> Zimmerman *et al.* developed copper-containing metal-organic nanoparticles for ppm level CuAAC reactions.<sup>13</sup>

<sup>a</sup>Advanced Materials Group, Materials Sciences and Technology Division, CSIR-North East Institute of Science and Technology, Jorhat, Assam – 785006, India.

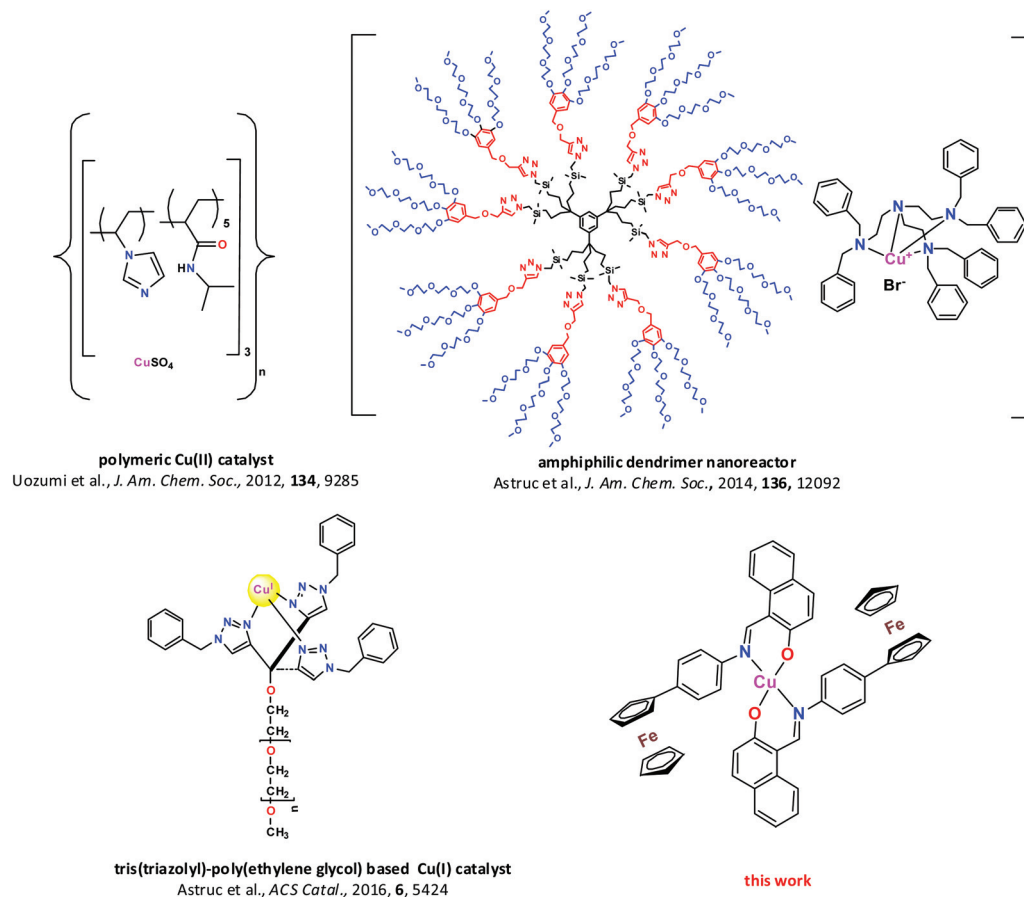
E-mail: bsaha@neist.res.in, bischem@gmail.com

<sup>b</sup>Academy of Scientific and Innovative Research (AcSIR), CSIR-NEIST Campus, Jorhat, Assam – 785006, India

<sup>c</sup>Advanced Computation Data Sciences Division, CSIR-North East Institute of Science and Technology, Jorhat, Assam – 785006, India

†Dedicated to Dr Dipak Kumar Dutta on the occasion of his 65th birthday.

‡Electronic supplementary information (ESI) available: Synthesis information, characterization studies, and spectra data. CCDC 1967275 1967276. For ESI and crystallographic data in CIF or other electronic format see DOI: 10.1039/d0dt00915f



**Scheme 1** Various ppm level copper catalysts for click reactions.

Lipshutz and co-workers devised iron-based Cu nanoparticles for an efficient ppm level catalysis of the click reaction.<sup>14</sup> Although these systems have enormous importance due to their low Cu loading (Scheme 1), there are still some difficulties associated with them. For instance, the complicated and time-consuming synthetic routes, *etc.*, inhibit their practical application. Therefore, the development of a simple and useful strategy for the CuAAC reaction with extremely low Cu-loading is of noteworthy interest. In this prospect, we wish to report herein the synthesis and characterization of a ferrocene-functionalized Schiff base containing a Cu(II) complex for ppm level catalysis in the CuAAC reaction under green condition.

## Results and discussion

### Synthesis and characterization of the ligand and metal complex

The Schiff base (**1**) was synthesized in an 85% (0.659 g) yield by refluxing 4-ferrocenyl aniline (0.500 g, 1.80 mmol, 1 equiv.) and 2-hydroxy-1-naphthaldehyde (0.526 g, 3.06 mmol, 1.7 equiv.) for 8 h in ethanol at 80 °C (Scheme 2). In the <sup>1</sup>H NMR spectrum of **1** in CDCl<sub>3</sub>, the azomethine proton showed a singlet at 9.28 ppm while the aromatic ring protons provided

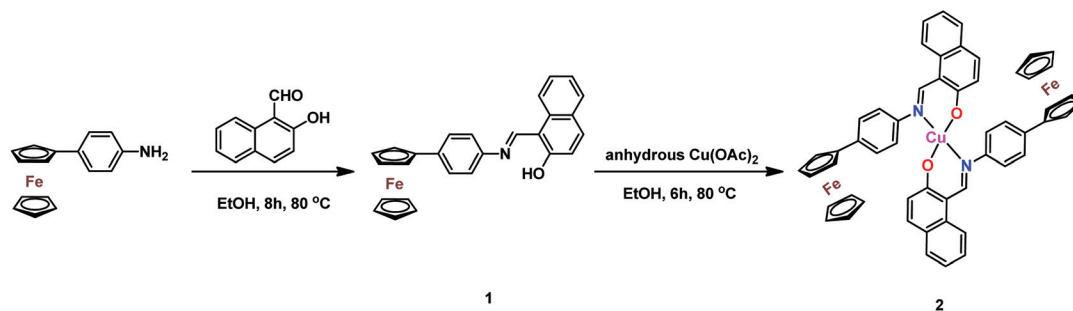
their signals in the range of 7.02–8.04 ppm (m, 10H) (Fig. S1, ESI†).

The unsubstituted ferrocenyl ring showed the characteristic singlet due to five chemically equivalent protons at 4.00 ppm while the substituted cyclopentadiene (Cp) ring peaks appeared at 4.61 and 4.29 ppm. The singlet at 15.56 ppm was attributed to the hydroxyl group. In the <sup>13</sup>C NMR spectrum of **1**, a signal at 170.7 ppm showed the azomethine carbon, and aromatic carbon atoms displayed their signals in the range of 108.7–142.4 ppm for the ligand (Fig. S2, ESI†). Furthermore, the peak observed at around 153.2 ppm was assigned to the C–N carbon. Carbon atoms of the substituted cyclopentadienyl ring appeared in the range of 69.1–69.5 ppm while those unsubstituted appeared at 66.3 ppm. A suitable crystal of **1** was grown under the slow evaporation of dichloromethane. The two Cp rings of ferrocene are staggered with each other (Fig. S3, ESI†). The C=N distance is 1.290(2) Å and that of OH⋯N is 1.765 Å.

The Schiff base ligand crystallized in a monoclinic crystal system with the *P21/c* space group.

Copper complex (**2**) was synthesized by refluxing anhydrous copper(II) acetate (0.181 g, 1 mmol, 1 equiv.) and **1** (0.862 g, 2 mmol, 2 equiv.) in ethanol for 6 h at 80 °C under a nitrogen atmosphere to give a 95% (0.876 g) yield (Scheme 2). The NMR





**Scheme 2** The synthesis of the ferrocene-functionalized Schiff base (**1**) and its copper(II) complex (**2**).

spectra of **2** could not be obtained due to its paramagnetic nature. The molecular structure of **2** reveals that two ligands coordinate to copper *via* the oxygen and nitrogen centres, forming a square planar geometry (Fig. 1). The ligands are *trans* to each other having O–Cu–O and N–Cu–N angles of 180° in both cases.

The cyclic voltammetric responses of **1** and **2** were recorded in dichloromethane solution containing 0.1 M Bu<sub>4</sub>NPF<sub>6</sub> (100 mV s<sup>−1</sup> scan rate) at 30 °C are shown in Fig. 2 and the corresponding electrochemical parameters are summarized in Table S1, ESI.† The observed anodic  $E_{1/2}$  values of **1** and **2** are close to the typical value for a pure ferrocene redox couple ( $0.45 \pm 0.02$  V on a GC electrode in dichloromethane), suggesting the oxidations are due to the Fe<sup>II</sup>/Fe<sup>III</sup> couple of the ferrocene moiety present in them. The higher positive reduction potential of **2** is due to the complexation of **1** with the Cu<sup>2+</sup> ion and the overall process remains one electron reversible for complex **2**.<sup>15</sup> We examined the origin of the redox behaviour by density functional theory (DFT) calculations. From the Frontier Molecular Orbitals (FMO) of **1** and **2**, it is also very clear that the electron pair in the Highest Occupied Molecular Orbital (HOMO) of **1** is more localized on the  $\pi^*$  orbitals of ferrocene (Fig. S4, ESI†), whereas in the

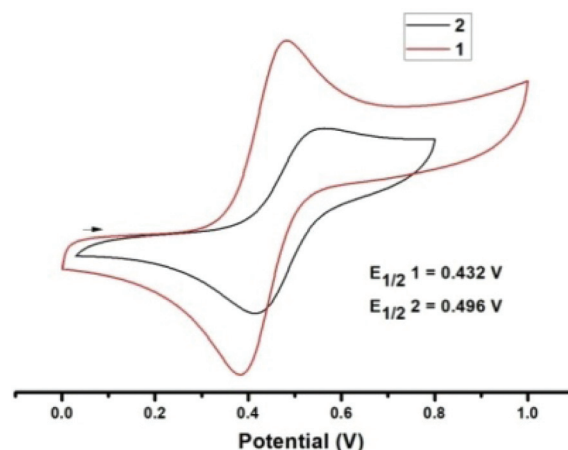


**Fig. 2** Cyclic voltammograms of **1** and **2**.

Singly Occupied Molecular Orbital (SOMO) of **2** there is an extensive mixing of the  $\pi^*$  orbitals of ferrocene with the  $\pi^*$  orbitals of the substituted Schiff base ligand (Fig. 4). Due to this extensive delocalization, the SOMO of **2** is stabilized from the HOMO of free ligand by 10 kJ mol<sup>−1</sup>. Interestingly, in cyclic voltammetry the anodic couple of **2** is shifted from that of **1** by 0.06 V towards a higher potential, supporting the fact.

The X-Ray Photoelectron Spectroscopy (XPS) spectra for the Fe and Cu metals of the metal complex are shown in Fig. 3. The Fe 2p<sub>3/2</sub> peak is observed at 707.98 eV, which is consistent with that of ferrocene (707.84 eV) and besides, the core level spectrum of Fe 2p<sub>1/2</sub> demonstrates a peak with a binding energy at 720.80 eV.<sup>16</sup> The peaks at 934.84 eV and 954.72 eV are attributed to the binding energies of 2p<sub>3/2</sub> and 2p<sub>1/2</sub> of Cu,

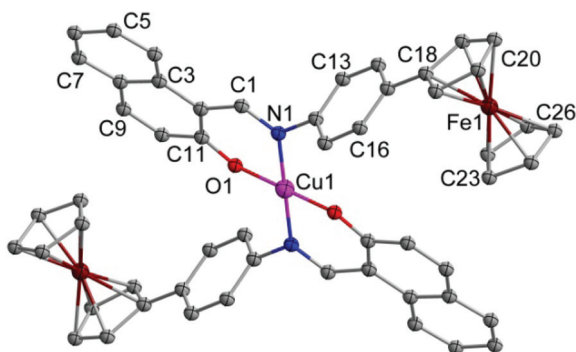


**Fig. 1** The molecular structure of **2** with important atoms labelled. Hydrogen atoms are omitted for clarity. Selected bond lengths [Å] and angles [°]: Cu1–O1, 1.8960(19); Cu1–N1, 1.999(2); Fe1–C18, 2.035(3); Fe1–C20, 2.043(3); Fe1–C23, 2.047(3); Fe1–C26, 2.040(3); O1–Cu1–N1, 89.41(8); N1–Cu1–N1, 180.0; and C26–Fe1–C20, 109.56(13). Symmetry code: 0.5 – X, 0.5 + Y, 0.5 – Z.

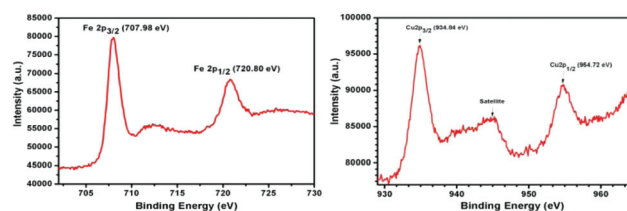


**Fig. 3** Fe 2p (left) and Cu 2p (right) XPS spectra of **2**.

respectively. In addition, the satellite peak observed at around 943 eV confirms the +2 oxidation state of copper in **2**.<sup>17</sup>

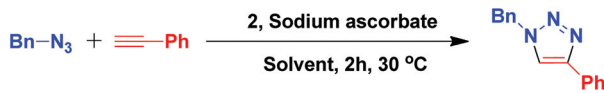
### Catalytic studies

Initially, the catalytic activity of **2** was tested in a model click reaction. 1 mmol benzyl azide and 1.2 mmol phenylacetylene were reacted in the presence of 2 mol% reducing agent, sodium ascorbate and 1 mol% **2** in aqueous media at 30 °C and 80% of 1,4-substituted triazole, *i.e.* 1-benzyl-4-phenyl-1*H*-1,2,3-triazole, was isolated after 2 h of the reaction (Table 1, entry 1). Different solvents were screened for this CuAAC cycloaddition reaction with 1 mol% **2** and 2 mol% sodium ascorbate for 2 h. Using various organic solvents, like THF, DMSO, DMF, acetonitrile and chloroform, led to low yields of the desired 1,2,3-triazole (entries 2–6). Furthermore, the (3 + 2) cycloaddition reaction in toluene furnished the triazole product in a 55% yield (entry 7). On the other hand, protic solvents, like methanol and ethanol, were also investigated in this transformation, leading to 60 and 65% yields, respectively (entries 8 and 9). Interestingly, a significant improvement of the yield was observed when the reaction was carried out in ethylene glycol (EG) (entry 10). Mixed solvents were also evaluated and we found that the best yield, 95%, was obtained in EG/H<sub>2</sub>O (entry 15), whereas in the DMSO/H<sub>2</sub>O, DMF/H<sub>2</sub>O, MeOH/H<sub>2</sub>O and EtOH/H<sub>2</sub>O systems, only 35, 40, 65, and 68% of products were isolated (entries 11–14). After ascertaining the EG/H<sub>2</sub>O mixture as the best solvent for this reaction, the catalyst was evaluated for its effective lowest level. It is worthwhile to mention that lowering the catalyst loading to 0.5 mol% (5000 ppm) and 0.1 mol% (1000 ppm) resulted in the same yield of 95% of the corresponding triazole (entries 16 and 17). Furthermore, the effective level of sodium ascorbate was determined and it was found that 1 mol% was sufficient for this transformation (entry 18). The reaction does not proceed in the absence of **2** or sodium ascorbate (entries 19 and 20). Under same reaction conditions, 1 mol% Cu(OAc)<sub>2</sub>·xH<sub>2</sub>O afforded 78% triazole product.<sup>18</sup>

The efficiency of the protocol was checked with a ppm level of catalyst loading using the same standard reaction of phenylacetylene and benzyl azide in the EG/H<sub>2</sub>O mixture (Table 2). Decreasing the catalyst loading to 50 ppm, the click reaction proceeds smoothly, affording the desired product in 92% yield with the TON and TOF of the catalyst at 18 400 and 9200 h<sup>−1</sup>, respectively (Table 2, entry 3). However, decreasing the catalyst level up to 20 ppm resulted in a moderate yield, 75%, of the product (entry 4). The highest 140 000 TON and 70 000 h<sup>−1</sup> TOF values were achieved with a 5 ppm loading of **2** and 70% of the desired triazole was isolated (entry 5). The rest of the click reactions were carried out with a 50 ppm catalyst loading of **2** and 1 mol% sodium ascorbate in EG/H<sub>2</sub>O (1 : 1) at 30 °C.

Phenylacetylene and benzyl azide were reacted in the presence of an excess amount of mercury metal with other standard conditions followed. After 2 h, 92% of the desired triazole product was isolated, which confirmed that the homogeneous path is maintained during the reaction.<sup>19</sup> The high catalytic activity of **2** is probably attributed to the presence of an extended  $\pi$ -conjugation in the Schiff base ligand and the attachment of the robust redox active ferrocene moiety enhances it further.<sup>20</sup> In the catalyst, the Schiff base fully covered the Cu(I) centre, which was generated by the reduction of **2** with sodium ascorbate, leaving a lack of free binding sites on the Cu(I) centre for possible destabilizing interactions.<sup>21</sup> Generally, Schiff base ligands are able to stabilize various oxidation states of transition metal ions<sup>22</sup> and in the CuAAC reaction it was necessary to control the stereoelectronic properties

**Table 1** Solvent and catalyst optimization studies<sup>a</sup>

				
Entry	<b>2</b> (mol%)	Sodium ascorbate (mol%)	Solvent	Yield <sup>b</sup> (%)
1	1.0	2.0	H <sub>2</sub> O	80
2	1.0	2.0	THF	25
3	1.0	2.0	DMSO	10
4	1.0	2.0	DMF	30
5	1.0	2.0	CH <sub>3</sub> CN	20
6	1.0	2.0	CHCl <sub>3</sub>	20
7	1.0	2.0	Toluene	55
8	1.0	2.0	MeOH	60
9	1.0	2.0	EtOH	65
10	1.0	2.0	EG	75
11	1.0	2.0	DMSO/H <sub>2</sub> O	35
12	1.0	2.0	DMF/H <sub>2</sub> O	40
13	1.0	2.0	MeOH/H <sub>2</sub> O	65
14	1.0	2.0	EtOH/H <sub>2</sub> O	68
15	1.0	2.0	EG/H <sub>2</sub> O	95
16	0.5	2.0	EG/H <sub>2</sub> O	95
17	0.1	2.0	EG/H <sub>2</sub> O	95
18	0.1	1.0	EG/H <sub>2</sub> O	95
19 <sup>d</sup>	—	1.0	EG/H <sub>2</sub> O	0
20	1.0	—	EG/H <sub>2</sub> O	0
21 <sup>c</sup>	1.0	2.0	EG/H <sub>2</sub> O	78

<sup>a</sup> Reagents and reaction conditions: Benzyl azide (1 mmol), phenylacetylene (1.2 mmol), the mentioned amount of **2** and sodium ascorbate in the given solvent were stirred at 30 °C in open air. <sup>b</sup> Isolated yield. <sup>c</sup> Cu(OAc)<sub>2</sub>·xH<sub>2</sub>O was used instead of **2**. <sup>d</sup> The reaction was carried out in new glassware using a new magnetic stir bar each time in triplicate without using **2**.

**Table 2** Click reaction between benzyl azide and phenylacetylene using ppm loading of **2**<sup>a</sup>

Entry	[ <b>2</b> ] (ppm)	Time (h)	Yield (%)	TON	TOF (h <sup>−1</sup> )
1	1000	2	95	950	475
2	100	2	94	9400	4700
3	50	2	92	18 400	9200
4	20	2	75	37 500	18 750
5 <sup>b</sup>	5	2	70	140 000	70 000

<sup>a</sup> All of the reactions were carried out with 1 mmol of benzyl azide, 1.2 mmol of phenylacetylene, the said amount of **2**, and 1 mol% sodium ascorbate in 1 mL of EG/H<sub>2</sub>O (1 : 1) at 30 °C. <sup>b</sup> 10 mmol of benzyl azide, 12 mmol of phenylacetylene, and 5 ppm of **2** were used in 10 mL of EG/H<sub>2</sub>O (1 : 1) and the rest of the conditions remained the same.

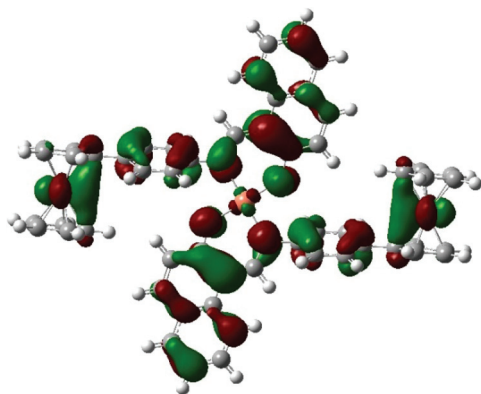


Fig. 4 The contour surfaces of the SOMO of **2**.

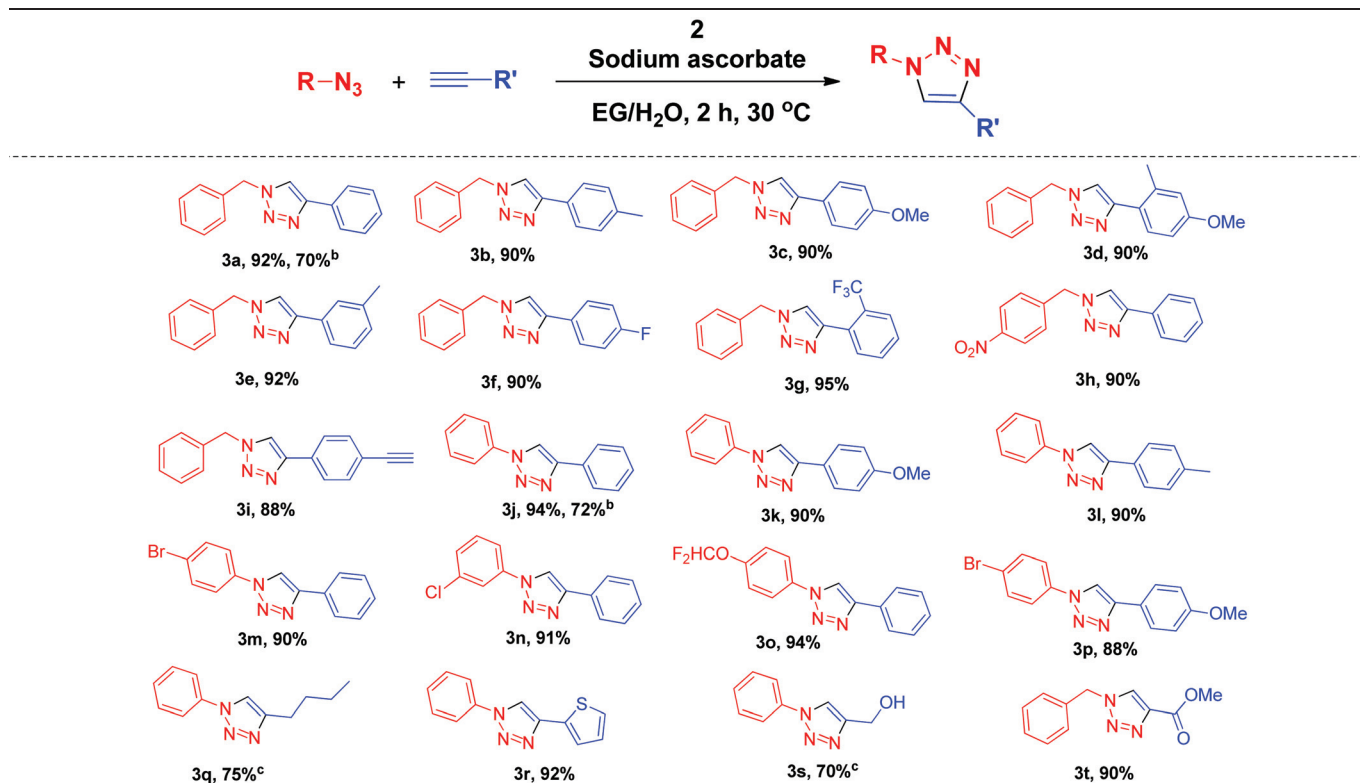
of the active Cu(I) species in the reaction medium. Besides, the precatalyst **2** also eliminated the need to handle the air sensitive Cu(I) compounds along with excess ligand/additives.<sup>7</sup> The formation of Cu(I) by the reduction of **2** with sodium ascorbate was monitored by UV-Vis spectroscopy (Fig. S5, ESI†). For Cu(OAc)<sub>2</sub>·xH<sub>2</sub>O, an absorption band in the range 700–800 nm was assigned to the characteristic metal d-d electronic transition.<sup>12</sup> The appearance of an intense band in the range between 300 and 400 nm of **2** was assigned to a metal to

ligand charge transfer (MLCT) transition, indicating Cu(I) in the complex. The phantom reactivity of magnetic stir bars due to metal contamination in the catalysis is one of the major consequences in catalysis.<sup>23</sup> So as to ensure the reactivity of **2**, a test experiment of the standard click reaction of phenylacetylene and benzyl azide under optimized condition was carried out using a new 25 mL round-bottomed flask equipped with a new magnetic stirring bar and to our delight the same result (92% yield) was obtained.

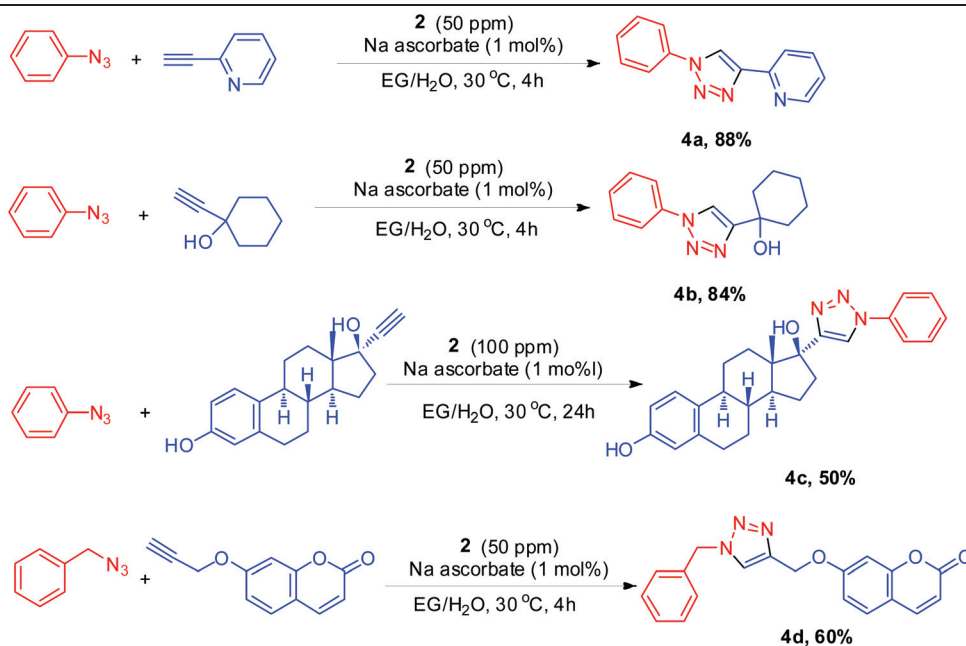
To know the extent of  $\pi$ -conjugation, DFT calculations at the B3LYP level of theory were carried out. The optimized structures have similar bond distances and angles as those of the molecular structure, which were determined on a single crystal (Table S3, ESI†). The presence of extended  $\pi$ -conjugation is confirmed in the SOMO of the optimized structure of **2** which is delocalized throughout the copper complex (Fig. 4).

With this encouraging result in hand, the scope of this low ppm level protocol was further explored for a variety of azides and alkynes (Table 3). As expected, all the reactions proceeded smoothly, leading to the desired 1,4-disubstituted 1,2,3-triazoles in good to excellent yields. Benzyl azide readily reacts with electron donating groups (4-Me, 4-OMe, 3-Me and 2-Me-3-OMe) of the substituted terminal aromatic alkynes, giving rise to the corresponding triazoles in yields of 90–92% (entries **3b**–

Table 3 Substrate scope of the azide–alkyne cycloaddition reaction using **2**<sup>a</sup>



<sup>a</sup> Conditions: Azide (1 mmol), alkyne (1.2 mmol), 50 ppm of **2** and sodium ascorbate (1 mol%) in EG/H<sub>2</sub>O (1 : 1) at 30 °C for 2 h in open air unless otherwise stated; yields of the products are given. <sup>b</sup> Gram scale synthesis using a 5 ppm loading of **2**. <sup>c</sup> Reaction time was 4 h.

Table 4 Application of **2** for the synthesis of different functional materials

**3e**). The reaction of electron-poor (2- $\text{CF}_3$ , 4-F) phenylacetylenes with benzyl azide proceeded easily to give the corresponding 1,2,3-triazoles in 90–95% isolated yield (entries **3f** and **3g**). Similarly, nitro substituted benzyl azide reacted readily with phenylacetylene, affording the desired product in excellent yield. Interestingly, the reaction of 1,4-diethynylbenzene with benzyl azide, affording alkynyl-containing 1,2,3-triazole, eliminates the need of a protecting group manipulation strategy, which can be applied in peptide ligation (entry **3i**).<sup>24</sup> On the other hand, aromatic azides also undergo an efficient conversion with various aromatic alkynes to form the target products in good to excellent yields (entries **3j–3p**). In the case of aliphatic alkynes, 1-hexyne smoothly underwent the reaction with phenyl azide, forming the cyclized products in a yield of 75% (entry **3q**). Moreover, heterocyclic alkynes, such as 2-ethynylfuran, were also tested in this (3 + 2) cycloaddition which led to the expected triazole product in excellent yield (entry **3r**).

Especially, functional groups, like hydroxyl and ester, were also tolerated under these conditions and could easily participate in this click reaction, affording good to excellent yield of the corresponding triazoles (Table 3, entries **3s** and **3t**). Gratifyingly, the gram scale reaction of benzyl azide (1.33 g, 10 mmol, 1 equiv.) and phenylacetylene (1.22 g, 12 mmol, 1.2 equiv.) furnished the 1-benzyl-4-phenyl-1*H*-1,2,3-triazole in a good yield (1.64 g, 70%) using only 5 ppm of this highly active catalyst. Similarly, 1,4-diphenyl-1*H*-1,2,3-triazole (**3j**) was synthesized in 72% isolated yield (1.59 g) from the reaction of phenyl azide (1.19 g, 10 mmol, 1 equiv.) and phenylacetylene (1.22 g, 12 mmol, 1.2 equiv.) using this efficient protocol.

In order to explore the applicability of this ppm level efficient protocol, different functionalized materials were successfully synthesized (Table 4). The bulk scale synthesis of pyridyl-1,2,3-triazole ligands is a lucrative proposition, as it is an alternative to the bipyridine and terpyridine ligands which have wide applications in the synthesis of functional metal complexes.<sup>25</sup> The reaction of phenyl azide and 2-ethynylpyridine under 50 ppm of catalyst loading gave 2-pyridyl-1,2,3-triazole in an 88% yield after 4 h (Table 4, entry **4a**). Similarly, 1-ethynylcyclohexanol, an active metabolite of the central nervous system depressant drug ethinamate,<sup>12</sup> readily reacts with phenyl azide, affording the targeted product in good yield (84%, entry **4b**). 17 $\alpha$ -Ethynyoestradiol, a synthetic orally bio-active oestrogen, is a derivative of the natural hormone, oestradiol, and used for the treatment of menopausal symptoms.<sup>10</sup> In this case, the reaction of 17 $\alpha$ -ethynyoestradiol with phenyl azide provided the desired triazole in 50% isolated yield (entry **4c**). Coumarin and its derivatives have found broad application in flavourings, perfumery, pesticides, fluorescent dyes as well as in medicinal chemistry.<sup>12</sup> In our study, the click reaction of 7-(prop-2-yn-1-yloxy)-2*H*-chromen-2-one offered the expected triazole product in a 60% isolated yield (entry **4d**).

## Conclusions

In summary, we have synthesized an air and moisture stable ferrocene functionalized Schiff base containing a Cu(II) complex and it was characterized *via* single crystal XRD and



spectroscopic techniques. Only a ppm level of copper catalyst is enough for the well-known Cu-AAC reaction, fulfilling the principles of a click reaction and green chemistry. With this convenient and easily accessible protocol, a wide range of 1,4-disubstituted 1,2,3-triazoles was synthesized in good to excellent yields. Furthermore, the gram scale synthesis, and biomedical and material science applications of this efficient catalytic system undoubtedly open exciting avenues for the scientific community.

## Experimental

Unless otherwise stated, all the reactions were performed in oven dried glassware under air. Chemicals were purchased from commercial suppliers (TCI, Alfa Aesar and Sigma-Aldrich) and used without further purification. Purification of the products was carried out by column chromatography using silica gel (200–300 mesh). Analytical thin-layer chromatography was performed using silica gel 60F<sub>254</sub> plates and visualization was carried out with UV light. <sup>1</sup>H NMR (500 MHz) and <sup>13</sup>C NMR (125 MHz) were recorded on a Bruker Avance 500 MHz spectrometer using TMS as an internal standard. Chemical shifts are reported in parts-per-million (ppm,  $\delta$ ) downfield from residual solvents peaks and coupling constants are reported as Hertz (Hz). Splitting patterns are designated as: s = singlet, d = doublet, t = triplet, q = quartet, m = multiplet, etc. UV-visible spectra were recorded on an UV-visible Spectrometer (Specord – 200, Analytik Jena) in the range of 200–800 nm. XPS spectra were recorded by an X-ray photo electron Spectrometer (ESCALAB Xi+, Thermo Fisher Scientific Pvt. Ltd, UK). The voltammetric analysis was carried out using a conventional three electrode system by using GAMRY Interface 1000E Potentiostat. FT-IR spectra were recorded on a PerkinElmer Spectrum 100 spectrometer with a KBr pellet in the frequency range of 4000–400 cm<sup>−1</sup>. HRMS were recorded on a Q-TOF spectrometer (Xevo XS QToF mass spectrometer) in electrospray ionization mode. Elemental analyses were conducted on a CHN analyser (PE-2400, PerkinElmer, USA).

### Synthesis of the ferrocene-based Schiff base (1)

The Schiff base **1** was synthesized by refluxing 4-ferrocenyl aniline (0.500 g, 1.80 mmol, 1 equiv.) and 2-hydroxy-1-naphthaldehyde (0.526 g, 3.06 mmol, 1.7 equiv.) for 8 h in absolute ethanol at 80 °C. After completion of the reaction, the orange yellow precipitate was filtered, washed several times with ethanol, dried under vacuum and recrystallized from dichloromethane. Yield 0.659 g (85%), M.p. 210–215 °C; FT-IR (KBr pellet, cm<sup>−1</sup>): 3480, 1620; <sup>1</sup>H NMR (500 MHz, CDCl<sub>3</sub>)  $\delta$ : 15.56 (s, 1H), 9.28 (s, 1H), 8.04 (d,  $J$  = 8.3 Hz, 1H), 7.73 (d,  $J$  = 9.1 Hz, 1H), 7.64 (d,  $J$  = 7.9 Hz, 1H), 7.47 (t,  $J$  = 9.0 Hz, 3H), 7.25 (t,  $J$  = 8.5 Hz, 3H), 7.02 (d,  $J$  = 9.1 Hz, 1H), 4.61 (s, 2H), 4.29 (s, 2H), 4.00 (s, 5H); <sup>13</sup>C NMR (126 MHz, CDCl<sub>3</sub>)  $\delta$ : 170.7, 153.2, 142.4, 138.1, 136.5, 133.1, 129.2, 127.9, 127.0, 123.3, 122.4, 120.1, 118.7, 108.7, 84.2, 69.5, 69.1, 66.3. HRMS (ESI-TOF-Q) calcd for C<sub>27</sub>H<sub>21</sub>FeNO: 431.0973, found: 431.0992

[M]<sup>+</sup>; Anal. Calcd for chemical formula: C<sub>27</sub>H<sub>21</sub>FeNO: C, 75.19; H, 4.91; N, 3.25. Found: C, 75.17; H, 4.89; N, 3.23.

### Synthesis of 2

The copper(II) complex bearing ferrocenyl Schiff base was synthesized by refluxing anhydrous copper(II) acetate (0.181 g, 1 mmol, 1 equiv.) and **1** (0.862 g, 2 mmol, 2 equiv.) in ethanol for 6 h at 80 °C under a nitrogen atmosphere. After cooling the reaction mixture to 30 °C, the brown colour precipitates were separated out from the mother liquor, washed with ethanol and dried well in high vacuo. Crystals suitable for X-ray structure analysis were obtained by recrystallization from dichloromethane. Yield 0.876 g (95%), M.p. 310–315 °C. FT-IR (KBr pellet, cm<sup>−1</sup>): 3393, 3053, 1599, 510, 415; Anal. Calcd for C<sub>54</sub>H<sub>40</sub>CuFe<sub>2</sub>N<sub>2</sub>O<sub>2</sub>: C, 70.18; H, 4.36; N, 3.03. Found: C, 70.16; H, 4.34; N, 3.01.

### Preparation of a stock solution of 2

In a 25 mL screw cap vial containing a magnetic stirrer bar, complex **2** (9.24 mg) was dissolved in 10 mL of THF and stirred for 10 min at 30 °C. A dark orange stock solution of **2** was obtained for the subsequent ppm level click reaction.

### General procedure for the azide alkyne cycloaddition reaction by 2

In a 25 mL round-bottomed flask equipped with a magnetic stirring bar, 46  $\mu$ L (50 ppm) of stock solution of **2** was added and THF was removed *in vacuo*. To this, 1 mmol organic azide, 1.2 mmol alkyne, 1.9 mg (1 mol%) of sodium ascorbate and 1 mL of EG/H<sub>2</sub>O (1 : 1) were added. The reaction mixture was stirred for 2 h at 30 °C under air. After 2 h, the mixture was extracted using EtOAc (3  $\times$  10 mL). The organic layer was dried over Na<sub>2</sub>SO<sub>4</sub> and the solvent was removed *in vacuo*. The crude product was purified *via* silica gel column chromatography using a gradient mixture of *n*-hexane and ethyl acetate to obtain the corresponding 1,2,3-triazoles.

**1-Benzyl-4-phenyl-1H-1,2,3-triazole (3a).** A 25 mL round bottom flask containing a magnetic stirring bar was charged with 46  $\mu$ L of stock solution, 5 ppm of **2** was added and THF was removed *in vacuo*. To this, benzyl azide (1.33 g, 10 mmol, 1 equiv.), phenylacetylene (1.22 g, 12 mmol, 1.2 equiv.), 1.9 mg (0.01 mmol) of sodium ascorbate and 10 mL of EG/H<sub>2</sub>O (1 : 1) were added. The reaction mixture was stirred for 2 h at 30 °C under air and, after completion, the mixture was extracted using EtOAc (3  $\times$  30 mL). The organic layer was dried over Na<sub>2</sub>SO<sub>4</sub> and the solvent was removed *in vacuo*. The residue was purified on silica gel (hexane/ethyl acetate) to furnish the 1-benzyl-4-phenyl-1H-1,2,3-triazole in 70% yield (1.64 g).

**1,4-Diphenyl-1H-1,2,3-triazole (3j).** The triazole **3j** was synthesized in a 72% isolated yield (1.59 g) utilizing phenyl azide (1.19 g, 10 mmol, 1 equiv.), phenylacetylene (1.22 g, 12 mmol, 1.2 equiv.), 1.9 mg (0.01 mmol) of sodium ascorbate, 5 ppm of **2** and 10 mL of EG/H<sub>2</sub>O (1 : 1) according to the procedure described for the gram scale synthesis of **3a**.



### X-ray data collection and refinement

Single-crystal X-ray studies were performed on a CCD Bruker SMART APEX diffractometer equipped with an Oxford Instruments low-temperature attachment. All the data were collected at 100(2) K using graphite-monochromated MoK $\alpha$  radiation ( $\lambda = 0.71073$  Å). The frames were indexed, integrated, and scaled by using the SMART and SAINT software packages<sup>26</sup> and the data were corrected for absorption by using the SADABS program.<sup>27</sup> The structures were solved and refined with the SHELX suite of programs.<sup>28</sup> All the hydrogen atoms were included in the final stages of the refinement and were refined with a typical riding model. Structure solution and refinement details for compounds **1** and **2** are provided in the ESI.† Anisotropic treatment of these three atoms resulted in nonpositive definite displacement tensors and were therefore subjected to isotropic refinement. Pertinent crystallographic data for compounds **1** and **2** are summarized in Table S2 in the ESI.† The crystallographic figures used in this manuscript were generated using Diamond 3.1e software.<sup>29</sup> CCDC-1967275 <http://www.ccdc.cam.ac.uk/cgi-bin/catreq.cgi> (1) and 1967276† <http://www.ccdc.cam.ac.uk/cgi-bin/catreq.cgi> (2), contain the supplementary crystallographic data for this paper.

### Computational study

Calculations were performed using density functional theory (DFT) with Becke's three-parameter hybrid exchange functional<sup>30</sup> and the Lee–Yang–Parr correlation functional (B3LYP).<sup>31</sup> Geometry-optimized structures were characterized fully *via* analytical frequency calculations as minima on the potential energy surface. The double- $\zeta$  basis set of Hay and Wadt (LanL2DZ) with effective core potential (ECP)<sup>32</sup> was used for Fe and Cu. The 6-31G(d,p) basis sets were used to describe the H, N, C, and O ligand atoms. All the optimization calculations were performed with the Gaussian 16 (G16)<sup>33</sup> suite of programs. The optimization of copper complex was performed in the gas phase.

### Conflicts of interest

There are no conflicts to declare.

### Acknowledgements

The authors are thankful for financial support from DST-SERB (ECRA and EEQ Project) and CSIR (FBR Project) New Delhi, India. FRG and DB thank SERB for fellowships ECR/2016/000849; GPP-0315 and EEQ/2017/000156; GPP-0333, respectively, and AAA and SR acknowledge CSIR-FBR project MLP-1010 for a scholarship. We are also grateful to the Director, CSIR-NEIST, for permission to carry out the work. Dr Sarat Ch. Patra and Sanjay Biswas are duly acknowledged for fruitful discussion about electrochemistry. We thank Prof. Dibyendu Mallick, Presidency University, Kolkata for his input into the DFT study.

### Notes and references

- (a) P. Thirumurugan, D. Matosiuk and K. Jozwiak, *Chem. Rev.*, 2013, **113**, 4905; (b) E. Bonandi, M. S. Christodoulou, G. Fumagalli, D. Perdicchia, G. Rastelli and D. Passarella, *Drug Discovery Today*, 2017, **22**, 1572.
- (a) A. Lauria, R. Delisi, F. Mingoia, A. Terenzi, A. Martorana, G. Barone and A. M. Almerico, *Eur. J. Org. Chem.*, 2014, 3289; (b) D. Dheer, V. Singh and R. Shankar, *Bioorg. Chem.*, 2017, **71**, 30.
- For selected reviews, see: (a) J. E. Moses and A. D. Moorhouse, *Chem. Soc. Rev.*, 2007, **36**, 1249; (b) H. Nandivada, X. Jiang and J. Lahann, *Adv. Mater.*, 2007, **19**, 2197; (c) J. E. Hein and V. V. Fokin, *Chem. Soc. Rev.*, 2010, **39**, 1302; (d) L. Liang and D. Astruc, *Coord. Chem. Rev.*, 2011, **255**, 2933; (e) S. G. Agalave, S. R. Maujan and V. S. Pore, *Chem. – Asian J.*, 2011, **6**, 2696; (f) D. Astruc, L. Liang, A. Rapakousiou and J. Ruiz, *Acc. Chem. Res.*, 2012, **45**, 630; (g) W. Xi, T. F. Scott, C. J. Kloxin and C. N. Bowman, *Adv. Funct. Mater.*, 2014, **24**, 2572; (h) C. S. McKay and M. G. Finn, *Chem. Biol.*, 2014, **21**, 1075; (i) E. Haldón, M. C. Nicasio and P. J. Pérez, *Org. Biomol. Chem.*, 2015, **13**, 9528; (j) S. Kahlal, J. Saillard and D. Astruc, *Coord. Chem. Rev.*, 2016, **316**, 1; (k) X. Wang, B. Huang, X. Liu and P. Zhan, *Drug Discovery Today*, 2016, **21**, 118; (l) A. H. El-Sagheer and T. Brown, *Acc. Chem. Res.*, 2012, **45**, 1258; (m) V. K. Tiwari, B. B. Mishra, K. B. Mishra, N. Mishra, A. S. Singh and X. Chen, *Chem. Rev.*, 2016, **116**, 3086.
- For selected reviews, see: (a) S. Hassan and T. J. Mueller, *Adv. Synth. Catal.*, 2015, **357**, 617; (b) C. G. Lima, A. Ali, S. S. van Berkel, B. Westermann and M. W. Paixão, *Chem. Commun.*, 2015, **51**, 10784; (c) H. B. Jalani, A. Ç. Karagöz and S. B. Tsogoeva, *Synthesis*, 2017, **49**, 29.
- (a) H. C. Kolb, M. G. Finn and K. B. Sharpless, *Angew. Chem., Int. Ed.*, 2001, **40**, 2004; (b) M. M. Trose, F. Nahra, D. B. Cordes, A. M. Z. Slawin and C. S. J. Cazin, *Chem. Commun.*, 2019, **55**, 12068.
- (a) V. V. Rostovtsev, L. G. Green, V. V. Fokin and K. B. Sharpless, *Angew. Chem., Int. Ed.*, 2002, **41**, 2596; (b) C. W. Tornøe, C. Christensen and M. Meldal, *J. Org. Chem.*, 2002, **67**, 3057.
- (a) E. Haldon, M. C. Nicasio and P. J. Perez, *Org. Biomol. Chem.*, 2015, **13**, 9528; (b) B. J. Borah, D. Dutta, P. P. Saikia, N. C. Barua and D. K. Dutta, *Green Chem.*, 2011, **13**, 3453; (c) S. Saha, M. Kaur and J. K. Bera, *Organometallics*, 2015, **34**, 3047.
- L. Liang, J. Ruiz and D. Astruc, *Adv. Synth. Catal.*, 2011, **353**, 3434.
- C. Deraedt, N. Pinaud and D. Astruc, *J. Am. Chem. Soc.*, 2014, **136**, 12092.
- Y. M. Yamada, S. M. Sarkar and Y. Uozumi, *J. Am. Chem. Soc.*, 2012, **134**, 9285.
- C. Deraedt, N. Pinaud and D. Astruc, *J. Am. Chem. Soc.*, 2014, **136**, 12092.

- 12 C. Wang, D. Wang, S. Yu, T. Cornilleau, J. Ruiz, L. Salmon and D. Astruc, *ACS Catal.*, 2016, **6**, 5424.
- 13 Y. Bai, X. Feng, H. Xing, Y. Xu, B. K. Kim, N. Baig, T. Zhou, A. A. Gewirth, Y. Lu, E. Oldfield and S. C. Zimmerman, *J. Am. Chem. Soc.*, 2016, **138**, 11077–11080.
- 14 A. Adenot, E. B. Landstrom, F. Gallou and B. H. Lipshutz, *Green Chem.*, 2017, **19**, 2506–2509.
- 15 M. Shabbir, Z. Akhter, I. Ahmad, S. Ahmed, M. Bolte, H. Ismail and B. Mirza, *Inorg. Chim. Acta*, 2017, **463**, 102.
- 16 Q. Dong, X. Zhuang, Z. Li, B. Li, B. Fang, C. Yang, H. Xie, F. Zhang and X. Feng, *J. Mater. Chem. A*, 2015, **3**, 7767.
- 17 J. Zhang, J. Yu, Y. Zhang, Q. Li and J. R. Gong, *Nano Lett.*, 2011, **7**, 4774.
- 18 C. Shao, G. Cheng, D. Su, J. Xu, X. Wang and Y. Hu, *Adv. Synth. Catal.*, 2010, **352**, 1587.
- 19 J. A. Widegren, M. A. Bennett and R. G. Finke, *J. Am. Chem. Soc.*, 2003, **125**, 10301.
- 20 (a) M. Bagherzadeh, H. Mahmoudi, S. Ataie, M. Hafezi-Kahnamouei, S. Shahrokhian, G. Bellachioma and L. Vaccaro, *Inorg. Chim. Acta*, 2019, **492**, 213; (b) H. Houjou, M. Ito and K. Araki, *Inorg. Chem.*, 2009, **48**, 10703; (c) X. Liu, N. Novoa, C. Manzur, D. Carrillo and J.-R. Hamon, *New J. Chem.*, 2016, **40**, 3308.
- 21 T. R. Chan, R. Hilgraf, K. B. Sharpless and V. V. Fokin, *Org. Lett.*, 2004, **6**, 2853.
- 22 For selected reviews, see: (a) M. Rezaeivala and H. Keypour, *Coord. Chem. Rev.*, 2014, **280**, 203; (b) C. J. Whiteoak, G. Salassa and A. W. Kleij, *Chem. Soc. Rev.*, 2012, **41**, 622; (c) J. Zhang, L. Xu and W. Y. Wong, *Coord. Chem. Rev.*, 2018, **355**, 180.
- 23 E. O. Pentsak, D. B. Eremin, E. G. Gordeev and V. P. Ananikov, *ACS Catal.*, 2019, **9**, 3070.
- 24 (a) V. Aucagne and D. A. Leigh, *Org. Lett.*, 2006, **8**, 4505; (b) T. Luu, B. J. Medos, E. R. Graham, D. M. Vallee, R. McDonald, M. J. Ferguson and R. R. Tykwinski, *J. Org. Chem.*, 2010, **75**, 8498; (c) I. Kim, K. C. Ko, W. R. Lee, J. Cho, J. H. Moon, D. Moon, A. Sharma, J. Y. Lee, J. S. Kim and S. Kim, *Org. Lett.*, 2017, **19**, 5509.
- 25 Q. V. C. van Hilst, N. R. Lagesse, D. Preston and J. D. Crowley, *Dalton Trans.*, 2018, **47**, 997.
- 26 *SAINT+software for CCD diffractometers*, Bruker AXS, Madison, WI, 2000.
- 27 G. M. Sheldrick, *SADABS Program for Correction of Area Detector Data*, University of Göttingen, Göttingen (Germany), 1999.
- 28 *SHELXTL Package v. 6.10*, Bruker AXS, Madison, WI, 2000; G. M. Sheldrick, *SHELXS-86 and SHELXL-97*, University of Göttingen, Göttingen (Germany), 1997.
- 29 K. Brandenburg, *Diamond, v3.1e*, Crystal Impact GbR, Bonn, Germany, 2005.
- 30 R. G. Parr and W. Yang, *Density-Functional Theory of Atoms and Molecules*, Oxford University Press, Oxford, UK, 1989.
- 31 (a) A. D. J. Becke, *J. Chem. Phys.*, 1993, **98**, 5648; (b) C. Lee, W. Yang and R. G. Parr, *Phys. Rev. B: Condens. Matter Mater. Phys.*, 1998, **37**, 785.
- 32 (a) P. J. Hay and W. R. Wadt, *J. Chem. Phys.*, 1985, **82**, 270; (b) W. R. Wadt and P. J. Hay, *J. Chem. Phys.*, 1985, **82**, 284; (c) P. J. Hay and W. R. Wadt, *J. Chem. Phys.*, 1985, **82**, 299.
- 33 M. J. Frisch, G. W. Trucks, H. B. Schlegel, G. E. Scuseria, M. A. Robb, J. R. Cheeseman, G. Scalmani, V. Barone, G. A. Petersson, H. Nakatsuji, X. Li, M. Caricato, A. V. Marenich, J. Bloino, B. G. Janesko, R. Gomperts, B. Mennucci, H. P. Hratchian, J. V. Ortiz, A. F. Izmaylov, J. L. Sonnenberg, D. Williams-Young, F. Ding, F. Lipparini, F. Egidi, J. Goings, B. Peng, A. Petrone, T. Henderson, D. Ranasinghe, V. G. Zakrzewski, J. Gao, N. Rega, G. Zheng, W. Liang, M. Hada, M. Ehara, K. Toyota, R. Fukuda, J. Hasegawa, M. Ishida, T. Nakajima, Y. Honda, O. Kitao, H. Nakai, T. Vreven, K. Throssell, J. A. Montgomery Jr., J. E. Peralta, F. Ogliaro, M. J. Bearpark, J. J. Heyd, E. N. Brothers, K. N. Kudin, V. N. Staroverov, T. A. Keith, R. Kobayashi, J. Normand, K. Raghavachari, A. P. Rendell, J. C. Burant, S. S. Iyengar, J. Tomasi, M. Cossi, J. M. Millam, M. Klene, C. Adamo, R. Cammi, J. W. Ochterski, R. L. Martin, K. Morokuma, O. Farkas, J. B. Foresman and D. J. Fox, *Gaussian 16, Revision C.01*, Gaussian, Inc., Wallingford CT, 2016.